Supplementary Material (ESI) for Chemical Communications

Supporting Information

A complementary palette of fluorescent silver nanoclusters

Jaswinder Sharma, Hsin-Chih Yeh, Hyojong Yoo, James H. Werner and Jennifer S. Martinez

Center for Integrated Nanotechnologies, Los Alamos National Laboratory, Los Alamos, NM-87545

S1. Time-resolved fluorescence lifetime analysis of AG4, AG3, AG2, AG1 nanoclusters and Cy5 attached to a single-stranded DNA are shown in Figure S1 (A)-(E) below. Fluorescence decay curves show the experimental data, the instrument response function (IRF), and the fit to one- or two-exponential models. Plots of weighted residuals for curve fitting are also included. Among these five fluorescent species, AG4 can be fit relatively well with a one-exponential model, while the rest are only fit with a two-exponential model. Both one- or two-exponential models convolved with a Gaussian instrument response function. All data fitting was done using the Levenberg-Marquardt least-squares method in Igor Pro (WaveMetrics). Photon arrival times with respect to the laser pulse were recorded using a photon counting module, PicoHarp 300, from PicoQuant.

S2. Fluorescence correlation spectroscopy (FCS) was performed on an inverted microscope (IX71, Olympus) using an oil immersion microscope objective (UPlanSApo 100x/1.40, Olympus). For measurements on Cy5-DNA and AG4 nanoclusters, 635 nm pulsed laser provided by a diode laser (model, PicoQuant) was used. A 488/632 dual-band dichroic (Chroma), a 725/150 band pass filter (FF01-725/150, Semrock), and a 75 μm diameter pinhole were used to spectrally and spatially filter the emission collected by the objective. A single-photon counting avalanche photodiodes (SPCM-AQR14, Perkin-Elmer) was used to collect the fluorescence emission. Collected photons were cross-correlated in a hardware correlator (ALV 5000E/FAST, ALV GmbH). At 4 kW/cm^2 of excitation power, the AG4 clusters and Cy5-DNA yielded detection rates greater than 90 kHz on the detector, well above the background emission from cluster- and Cy5-free phosphate buffer (<1 kHz). As a result, the autocorrelation functions of the clusters were not influenced by the background emission. The autocorrelation functions were fit to the following 2D model with one triplet state:

$$G(\tau) - 1 = \frac{1}{N}\left(1 + \frac{\tau}{\tau_d}\right)^{-1}\left(\frac{1 - F + F \cdot \exp\left(-\frac{\tau}{\tau_r}\right)}{1 - F}\right)$$

where G is the autocorrelation function and τ is the lag time. N is the average number of the fluorescent molecules residing in the detection volume. τ_d and τ_r are the characteristic diffusion time and blinking time constants, respectively. F is the effective fraction of molecules in non-fluorescent states. All data fitting was done using the Levenberg-Marquardt least-squares method in Igor Pro (WaveMetrics). Table S1 shows the parameters used to fit the autocorrelation curves of AG4 clusters and Cy5-DNA. Diffusion time constants, τ_d, of 9.56 ms for the TetraSpeck™ blue/green/orange/dark red beads (Invitrogen) were obtained for diffusion in aqueous solution. By use of the size of these TetraSpeck beads (diameter 110 nm), we estimated the diameter of

the detection volume to be 0.77 μm, allowing us to estimate the physical values such as diffusion coefficient and hydrodynamic size for both of these fluorophores.

Table S1. An example of parameters used in FCS curve fitting.

	N	τ_d (ms)	F	τ_r (μs)	Count rate (kHz)
AG4	8.20	0.52	0.64	2.7	190.1
Cy5-DNA	4.53	0.18	0.36	14.2	147.8

	Counts per fluorophore (kHz)	D ($\mu m^2/s$)	R_h (nm)
AG4	23.2	71.5	3.00
Cy5-DNA	32.6	202.4	1.06

Excitation density was at 4.27 kW/cm^2.
D: Diffusion coefficient ($\mu m^2/s$)
R_h: Hydrodynamic radius (nm).

S3. Excitation power-dependent blinking dynamics of AG4 and Cy5-DNA were illustrated in Fig. S2 (a-c). Blinking is a photoinduced process, with the rate constant highly dependent on the excitation power.

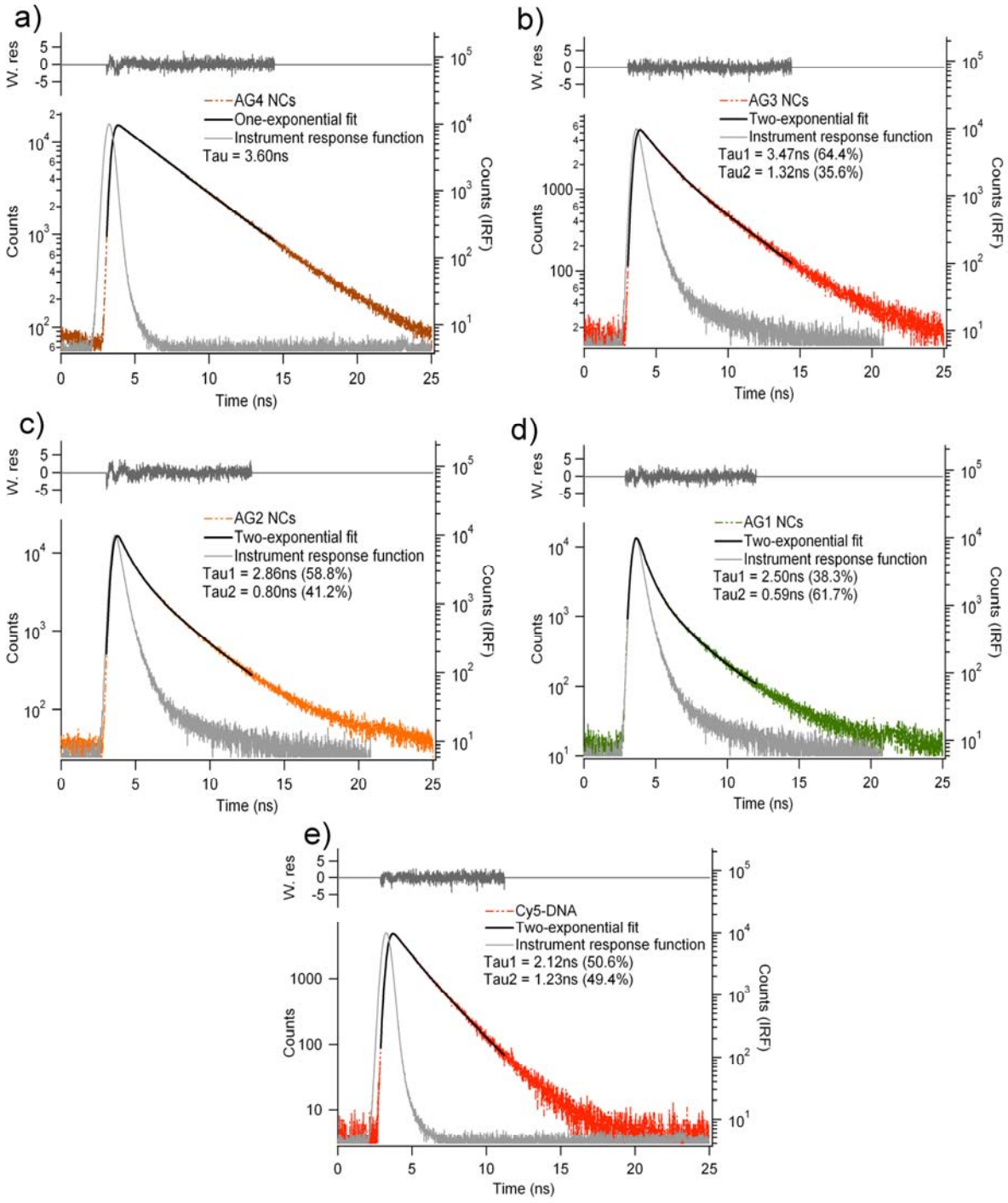

Fig. S1. Time-resolved fluorescence lifetime analysis of (a) AG4, (b) AG3, (c) AG2 , (d) AG1, and (e) Cy5 attached to a single-stranded DNA, respectively. The reduced chi-square values (χ^2) for each fit are: 1.37, 1.32, 1.36, 1.40, and 1.04 from A to E, respectively. The pulsed laser source and the filter used for each fluorophore are: (a) 635 nm, Semrock FF01-725/150, (b) 437 nm, Semrock FF01-641/75, (c) 437 nm, Semrock FF01-607/70, (d) 437 nm, Semrock FF01-550/88, and (e) 635 nm, Chroma Technology 670DF.

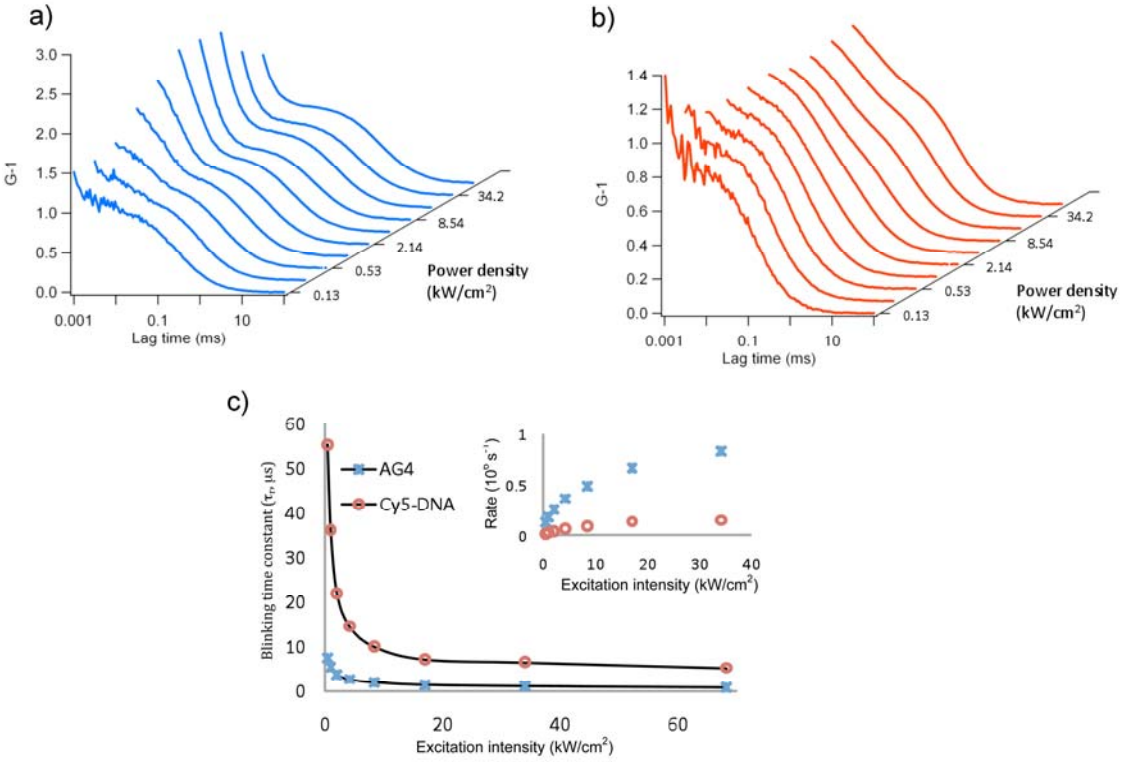

Fig. S2. (a) Waterfall plots of FCS autocorrelation curves of AG4 with different excitation power density. Blinking dynamics (τ_r = 7.6 μs) are clearly seen at power density greater than 0.53 kW/cm^2. (b) FCS autocorrelation curves of Cy5-DNA at different excitation power density. Blinking dynamics (τ_r = 14.2 μs) become obvious when the power density is greater than 4.27 kW/cm^2. (c) Blinking time constants (τ_r, in μs) of AG4 and Cy5-DNA under various excitation power densities, as estimated by FCS. The inset shows the blinking rates ($k_r = 1/\tau_r$, 10^6 s^{-1}) of AG4 and Cy5-DNA versus excitation intensity.

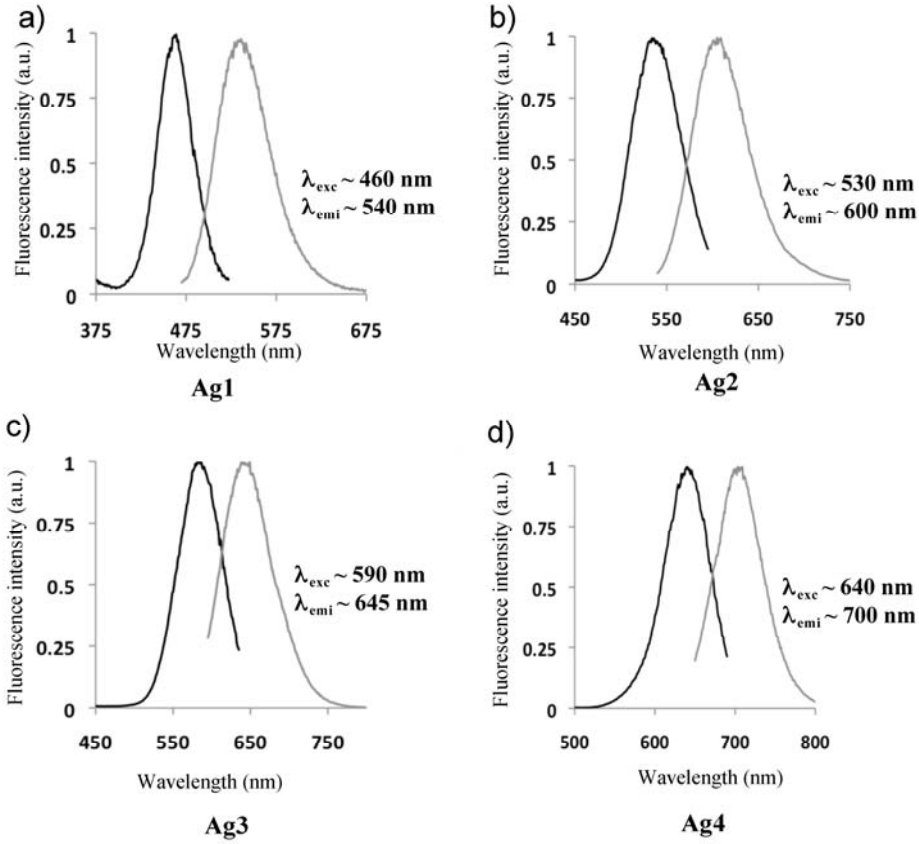

Fig. S3. Excitation and emission spectra for nanoclusters synthesized in water using sequences Ag1 (a), Ag2 (b), Ag3 (c), and Ag4 (d).

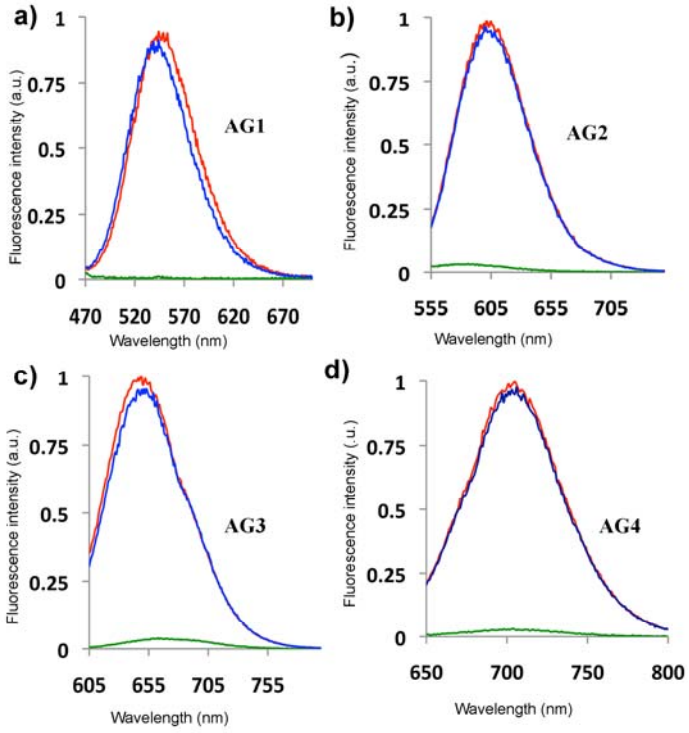

Fig. S4. Reversibility of fluorescence on addition of $NaBH_4$. (a) AG1 nanoclusters, (b) AG2 nanoclusters, (c) AG3 nanoclusters, and (d) AG4 nanoclusters. For each figure, red represents the fluorescence for the as synthesized cluster, green represents the oxidized cluster (higher oxidation state in case of AG1) and blue represents the rereduced cluster.

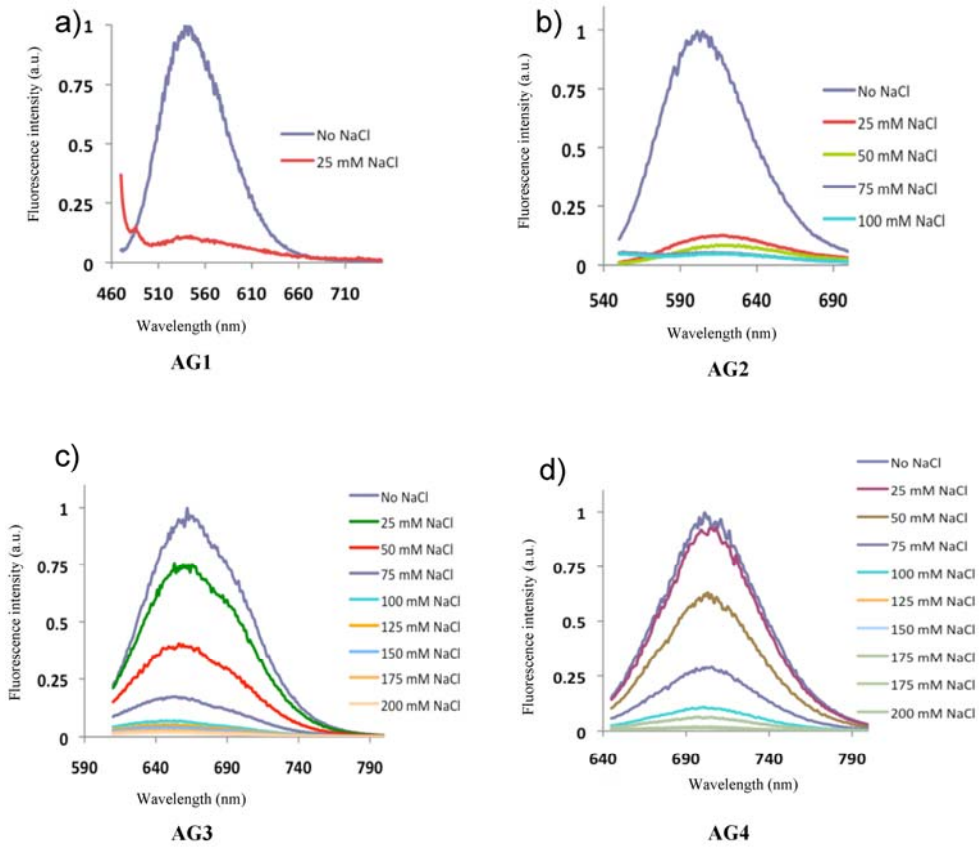

Fig. S5. The effect of NaCl concentration on the fluorescence intensity of nanoclusters. (a) AG1, (b) AG2, (c) AG3, and (d) AG4.

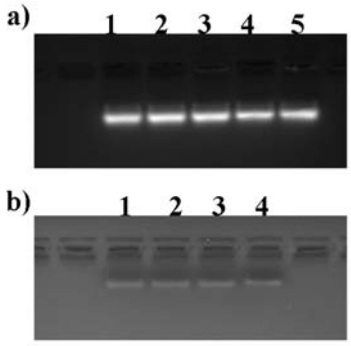

Fig. S6. Control experiments showing the lack of non-specific binding for AG4 nanoclusters (long DNA strand) with protein molecules. a) Lane 1: ag4 DNA; Lane 2: AG4 nanoclusters; Lane 3: AG4 + streptavidin; Lane 4: AG4 + BSA; Lane 5: AG4 + PDGF (2% agarose gel 2% stained with ethidium bromide) b) Lane 1: AG4 nanoclusters; Lane 2: AG4 + streptavidin; Lane 3: AG4 + BSA; Lane 4: AG4 + PDGF (2% agarose gel having no ethidium bromide. Bands are visible due to nanocluster fluorescence). (in both cases AG4 were incubated with different proteins for 1hr in phosphate buffer (pH~7, 20 mM)

S4. Effect of time on photoemission spectra evolution and stability of nanoclusters with respect to light, temperature and air.

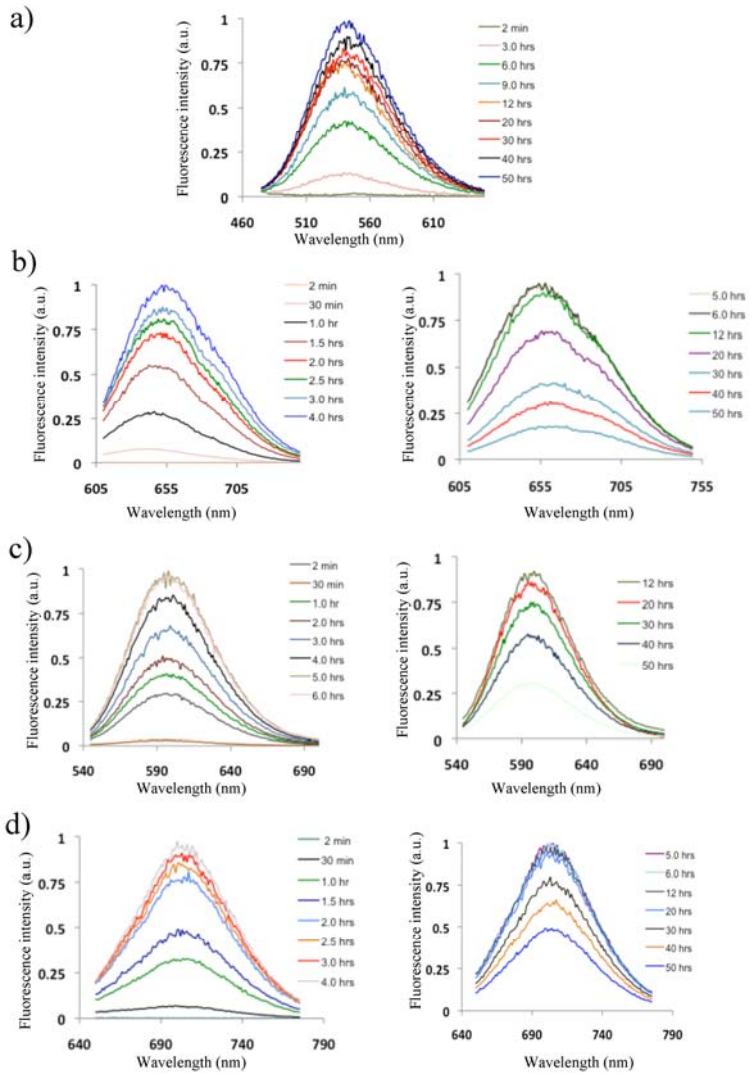

Fig. S7. Effect of time on photoemission spectra of nanoclusters. a) AG1 b) AG2 c) AG3 and d) AG4.

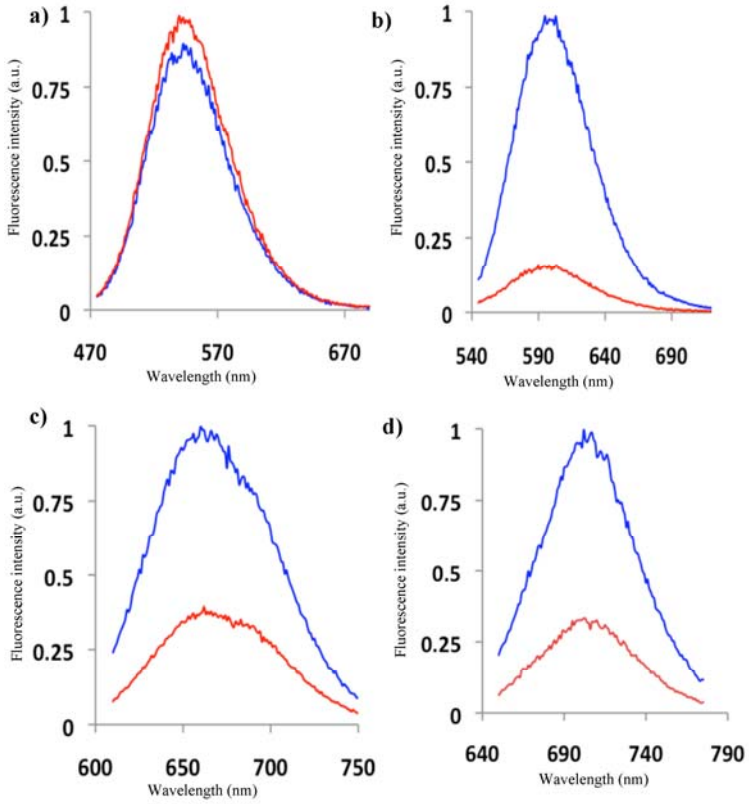

Fig. S8. Effect of ambient light on nanocluster stability. a) AG1 b) AG2 c) AG3 and d) AG4. (spectra were taken after placing the nanoclusters in light (red) or dark (blue) for 12 hrs.

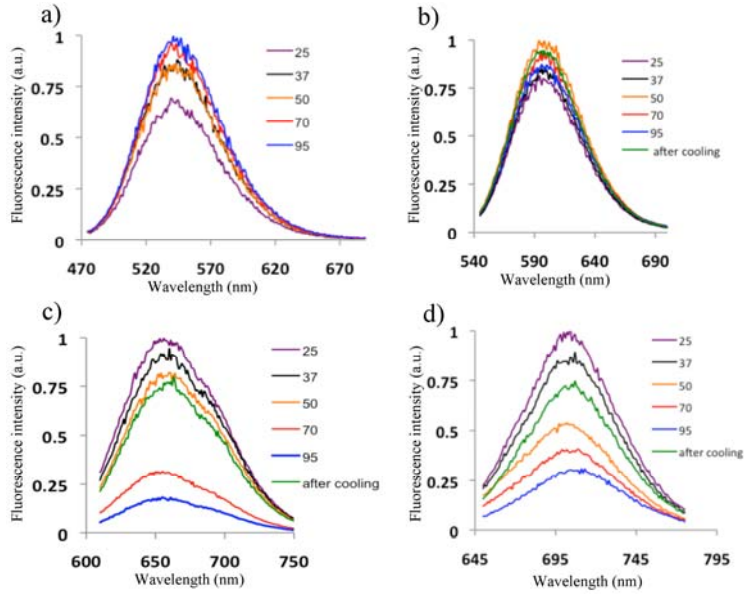

Fig. S9. Effect of temperature (°C) on nanocluster stability. a) AG1 b) AG2 c) AG3 and d) AG4. (Preformed nanoclusters were incubated at indicated temperature for five minutes prior to taking the spectrum. After the final incubation at 95°C, the clusters were cooled to room temperature and a final spectrum was taken.)

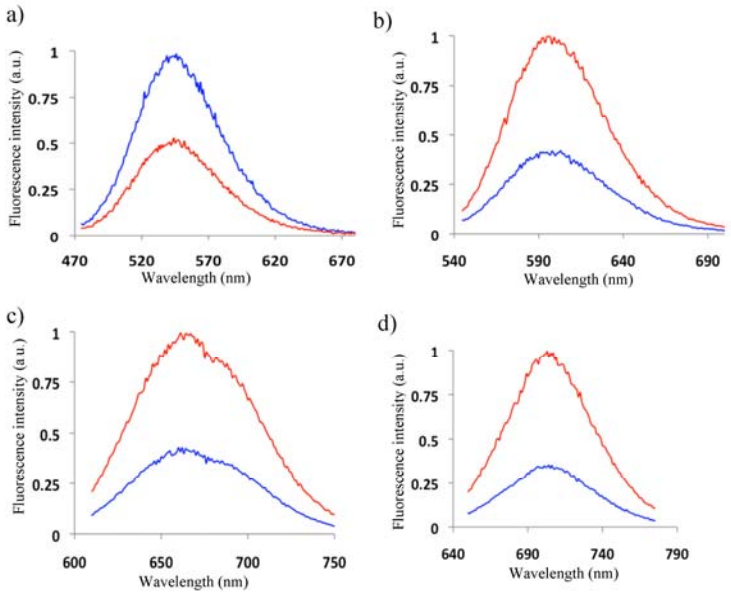

Fig. S10. Effect of air (oxygen) on nanocluster stability. a) AG1 b) AG2 c) AG3 and d) AG4. (Nanoclusters were synthesized in air and after four hours divided into two. One aliquot was placed in argon (red), the other in ambient air (blue). Spectra were taken after 50 hours.)

From studies of oxygen, light and temperature effects on the nanocluster stability, it appears that AG2, 3, and 4 are synthesized as the reduced species and oxidized over time. In contrast to that observed for AG1, which over time appears to convert to a non-emissive higher oxidative state.

In case of AG2, fluorescence emission increases as a function of temperature up to 50 °C, but then slightly decreases at higher temperatures. Stability of nanoclusters having longer DNA sequence decreases with increase in temperature showing that the surrounding DNA sequence is playing a role in the photoemission of nanoclusters, which with increase of temperature may unwrap from the nanoclusters and hence lead to a decrease in fluorescence; however even at 95 °C nanoclusters retain some fluorescence. Also, we observed on cooling that nanoclusters, especially with longer DNA sequences, regain their fluorescence, which proves that the surrounding DNA sequence plays a role in the enhanced fluorescence emission of these nanoclusters, which unwraps at higher temperatures and wraps the nanoclusters again at lower temperatures. This cooling reheating cycle can be observed multiple times without loosing fluorescence emission.

From all the above studies, we assume that the photophysical properties of the nanoclusters are not only controlled by the number of atoms present in the nanocluster, but the surrounding DNA sequence and the oxidation state of the nanoclusters also plays a role in determining their photoemission intensity and in some cases emission wavelength (most of the green emitting species are considered as the oxidized species).[1]

References:

1. C. M. Ritchie, K. R. Johnsen, J. R. Kiser, Y. Antoku, R. M. Dickson and J. T. Petty, *J. Phys. Chem. C,* 2007, **111**, 175